

Geochemical Distribution of Heavy Metals and Assessment of Environmental Indicators in Chah-Shaljami Polymetal Ore deposit, South of Birjand, Iran

Rahim Dabiri^{1*}, Heydar Hagdoust¹, Reza Arjmandzadeh²

¹ Department of Geology, Mashhad Branch, Islamic Azad University, Mashhad, Iran

² Department of Geology, Payame Noor University (PNU), P.O.BOX 19395-3697 Tehran, Iran

*Corresponding author, e-mail: r.dabiri@mshdiau.ac.ir

(received: 13/06/2018 ; accepted: 07/08/2018)

Abstract

The Chah-Shaljami polymetal ore deposit contains heavy metal anomalies in various mineralization zones. Geochemical distribution and correlation of elements in surficial soils indicate that sulfide, sulfate, sulfosalt and silicate mineral occurrences (e.g. Pyrite, chalcopyrite, galena, sphalerite, molybdenite, enargite, hornblende and biotite) in mineralization and stockwork zones resulted in the strong correlation between some elements such as Fe, Mn, Mg, Ni, Pb, Zn, Cr and Sn. In addition, there is a relatively strong correlation between Cd, Ti, Ba, Al which may be related to the vein-veinlets and the intrusives. Contamination indexes (enrichment factor, geoaccumulation index (Igeo), contamination factor and modified contamination degree) were used to assess the soil and sediment enrichment in Chah-Shaljami ore deposit. These indexes indicate enrichment of S, Sb, Mn, Pb. Sulfide, sulfate and sulfosalt minerals cause strong sulfur enrichment. Cadmium is weakly contaminated as can be inferred from its paragenetic association with Pb-Zn minerals in polymetal ore deposits.

Keywords: Chah-Shaljami, Heavy Metal, Stockwork, Enrichment Factor, Contamination.

Introduction

Heavy metals and metalloids are of crucial combinations in entire sorts of soils and a significant constituent of clays and Fe and Al oxides (Violante *et al.*, 2010). Distribution of heavy metals in soil is inherited from parent material which are shifting through the systematic cycle of rock-soil-plant in an unabated fashion. Soil texture, clay content, pH and Fe and Al oxides are among the most considerable features of soils, playing a crucial role in dynamism and biologic adsorption of heavy metals (Kabala & Singh, 2001). Rise in their concentration might be triggered through lithogenic procedures or anthropogenic activities (Febles *et al.*, 2014). Ore deposits and mining are important due to bearing a plethora of anomalies. Heavy metals have significant ecological importance due to high stability in environment and gathering in some natural reservoirs. Natural phenomena such as alteration, weathering and erosion across the areas of mining potential can also impose destructive impacts on environment and contaminate water and soil resources. The objectives of the present study are: (a) to assess the level of metal pollution in Chah-Shaljami polymetal ore deposit using geochemical indices, such as enrichment factor (EF), geoaccumulation index (Igeo), contamination factor (CF) and modified contamination degree (mCd); and (b) to analyze

possible sources of metals in Chah-Shaljami polymetal ore deposit using multivariate cluster analysis diagram (CA) and principal component analysis (PCA).

Geological setting

The magmatism in the Lut Block, which is represented by a wide range of volcanic (both effusive and pyroclastic) and intrusive rocks, started in the Late Jurassic, with the intrusion of Shah-Kuh batholith, and continued until the Quaternary (Arjmandzadeh & Santos, 2014). Chah-Shaljami prospect is located 190 km to the south of Birjand in the Lut Block volcanic-plutonic belt (Figure 1). It is an extensive broadly circular alteration zone hosted by andesitic rocks (Figure 2). Although located only a few kilometers from Qalehzari copper-gold-silver deposit, the two localities do not seem to have any direct genetic connection (Arjmandzadeh *et al.*, 2011). The igneous bodies in the Chah-Shaljami area consist mainly of lava flows, pyroclastic deposits, dykes and stocks. Volcanic rocks in Chah-Shaljami are crystal tuff, green tuff, basalt, andesitic basalt and andesite, which are highly altered in the central parts of the area. According to Rb-Sr dating, the volcanics have a 40.5 ± 2 Ma age (Kluyver *et al.*, 1978).

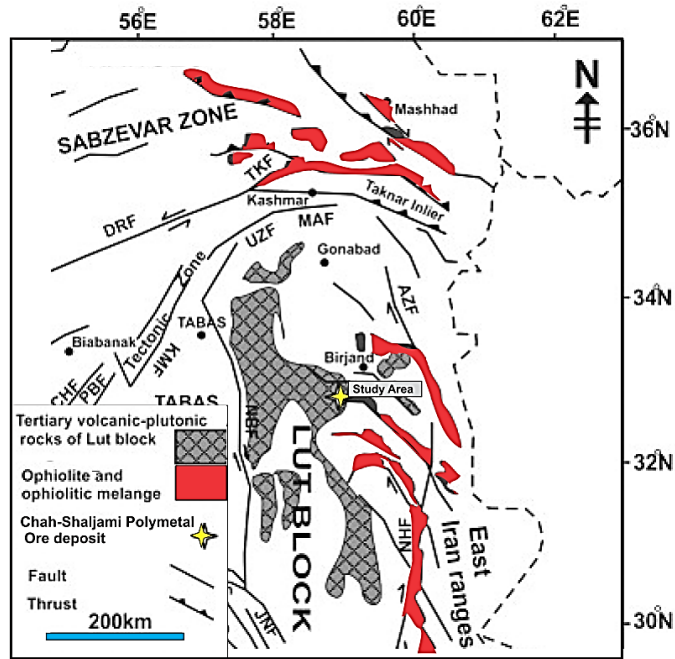


Figure 1. General tectonic map of East Iran and tectonic setting of the Lut Block in eastern Iran. Several major faults are shown: DRF: Doruneh Fault, TKF: Taknar Fault, MAF: Mehdiabad Fault, UZF: Uzbak-Kuh Fault, NHF: Nehbandan Fault, KMF: Kalmard Fault, AZF: Abiz Fault. (modified after Shafaroudi *et al.* (2015)).

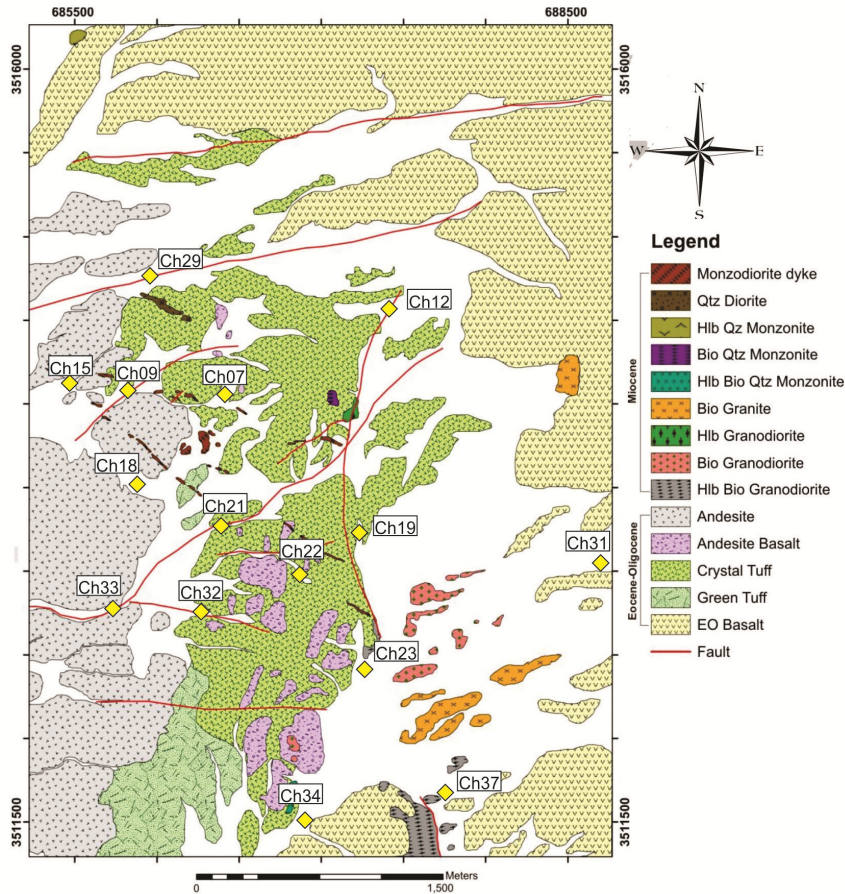


Figure 2. The geological map of Chah-Shaljami area (after Arjmandzadeh *et al.* (2010) and sampling location.

Petrographic studies on Chah-Shaljami sub-volcanics indicate that they comprise quartz monzodiorite dyke, hornblende granodiorite dyke, pyroxene hornblende biotite quartz monzonites, hornblende biotite quartz monzonites, hornblende quartz monzonites, biotite quartz monzonites, quartz monzonites, hornblende biotite granodiorites, biotite granodiorites. The Chah-Shaljami alteration zone is believed to be an advanced argillic lithocap marking the shallow parts, hosted by the volcanics, of a porphyry copper system (Karimpour *et al.*, 2014). Arjmandzadeh *et al.* (2010) detected some anomalies of heavy elements, such as Pb, Sb, As, Cu and Zn within the siliceous, sulphide and stockwork veinlets. These anomalous areas have As contents up to 401 ppm, Pb, 240 ppm and Zn, 47 ppm. The stockwork of chalcopyrite–galena–sphalerite is also present. Mineralisation is poorly developed in quartz-alunite zone however, the occurrence of some malachite and pyrite is reported.

Materials and methods

Before field reconnaissance, ASTER data were processed using colour compositions of band ratios, principal component analysis, selective principal components analysis (SPCA) and spectral angle mapping to investigate and distinct different alteration zones. After processing ASTER data, 22 samples were collected from surficial soils around

the deposit during the dry month of Jun 2013. The locations are represented in Figure. 2. Some 10 gr of samples were analyzed at Zar-Azma Laboratory to determine heavy metal contents using ICP- MS approach. The results of geochemical analysis are presented in Table 1. Moreover, to determine the distribution of heavy metals in soil around the deposit and to investigate the impact of contamination, indices of contamination and environment, contamination factor (CF), modified coefficient of contamination (mCd), enrichment factor (EF) and the geoaccumulation index (Igeo) were calculated that are proposed by USEPA (2002).

Discussion

Remote sensing

The Reflectance behavior of alteration-mineralisation zones and soils varies depending on the vegetation, mineralogical features, soil colour, superficial moisture, organic material, particle size, heavy metals, soil roughness, drainage characteristics and the residual sediments. Additionally, there are great relationships between alteration, mineralisation and geochemical concentration of heavy elements.

Alteration-mineralisation mapping of an area by means of satellite data profoundly help analyse the environmental issues.

Table 1. The geochemical composition of elements of soil and sediments of Chah-Shaljami polymetal deposit.

sample	As	Ca	Cd	Co	Cr	Cu	Fe	Mg	Mn	Mo	Na	Ni	Pb	Sn	Sr	Ti	v	Zn	Al	Ba
DL	0.1	100	0.1	1	1	1	100	100	5	0.1	100	1	1	0.1	1	10	1	5	100	1
Unit	ppm	ppm	ppm	ppm	ppm	ppm	ppm	ppm	ppm	ppm	ppm	ppm	ppm	ppm	ppm	ppm	ppm	ppm	ppm	ppm
CH07	10.3	10113	0.14	12.1	25	32	9507	1241	119	1.54	10045	18	20	0.4	3498.8	1676	67	12	24852	75
CH09	17.2	85235	0.76	15.1	94	37	37596	17783	745	1.26	14059	49	24	2	479.1	5343	131	76	77413	471
CH12	11.9	73585	0.72	14.6	114	97	36815	15619	767	1.01	14434	48	27	2.7	391	5557	127	105	64959	357
CH15	19.3	72212	0.72	13.8	91	40	34682	15564	719	1.9	13773	46	24	1.7	411.9	5062	118	73	66774	367
CH18	14.7	73044	0.82	13	97	41	37253	13941	636	1.37	13682	43	26	2.2	455.7	4980	128	71	64004	369
CH19	9.2	13048	1.18	2.9	46	6	3357	885	15	1.07	3383	3	19	1.3	399	5652	142	12	91243	646
CH21	13.9	74798	0.88	15	100	48	38527	15451	830	0.84	14882	47	25	2.1	384.1	6123	136	84	61822	370
CH22	11.6	80140	0.91	14.7	109	52	39264	15917	804	1.3	14169	49	26	2.4	568.2	5812	138	86	63932	370
CH23	11.6	76429	0.91	15.2	89	44	35809	16679	809	1.47	14202	52	25	1.9	384.2	5424	121	82	65521	339
CH29	9.2	75790	0.87	15.4	121	57	39334	16483	865	0.76	14653	50	28	2.6	491.7	5968	142	92	65372	359
CH31	18.8	68800	0.65	14.4	106	38	42127	15029	687	0.9	14731	45	22	1.7	411.9	5199	137	71	67330	338
CH32	11.5	71079	0.86	15.4	120	39	37158	16051	782	0.76	14331	50	24	1.8	355.1	5542	130	79	64781	338
CH33	12.2	75811	0.72	14.8	95	47	37175	16761	799	1.08	14864	49	29	2.3	404.8	5407	128	83	66657	359
CH34	13.2	73661	0.69	15	106	56	37713	16604	780	1.11	14000	50	29	2.6	389.5	5272	123	90	65988	341
CH37	18.1	72640	0.59	15.6	84	62	35213	17899	764	0.97	13771	53	28	3.2	408.1	4746	117	89	70631	383
CH BLANK	14.2	77831	0.77	14.4	110	43	38716	16461	839	0.57	13658	49	28	2.7	376.1	6066	138	83	63592	346

The principal alteration halo is, through the processing of ASTER data, broad and elliptical of 3×4 km (Figure 3). To distinguish the distinctive alteration-mineralization zones using (SAM) spectral angle mapper methodology, the USGS spectrum diagrams of proposed minerals were employed as the reference data/database. The index minerals of high-sulphidation epithermal deposits consist of alunite, jarosite, chlorite, dickite, sericite, montmorillonite, quartz and Fe-oxides. Mineralisation in sericite zone consists of pyrite+ molybdenite +anargite (Figure. 4). Moreover, the veinlets of chalcopyrite are scattered within quartz- dickite-pyrite zone, have partly transformed into malachite.

Correlation analysis

In order to determine the relationship among elements, the Pierson's coefficient of correlation is measured (Table 2). Obviously, most of metals incorporated in the Table, have strong to medium correlation. For instance, there are positive and meaningful correlations among Fe and Mn ($r=0.962$, $P<0.01$) as Mg ($r=0.957$, $P<0.01$), Ni ($r=0.955$, $P<0.01$), Pb ($r=0.712$, $P<0.01$), Zn ($r=0.918$, $P<0.01$), Cr ($r=0.900$, $P<0.01$) and Sn ($r=0.685$, $P<0.01$). Fe-bearing (e.g. pyrite, chalcopyrite and jarosite) and Pb- and Zn-bearing minerals (e.g. galena, cerussite and sphalerite) formed in stockwork zone (Arjmandzadeh *et al.*, 2010).

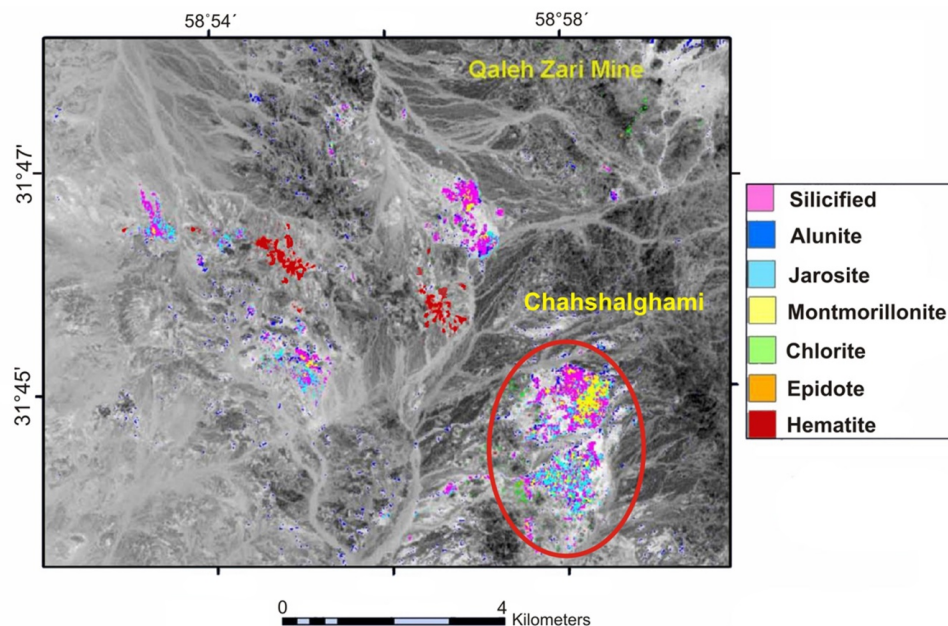


Figure 3. The result of SAM classification for alteration minerals in Chah-Shaljami polymetal ore deposit.



Figure 4. The aggregate of elongated and subhedral crystals of molybdenite (XPL).

Quite high correlation degree among the foregoing elements highlights their joint source (strockwork zones). Moreover, Cd displays a meaningful relationship with Ti ($r=0.838$, $P<0.05$), Ba ($r=0.835$, $P<0.05$) and Al ($r=0.812$, $P<0.05$) which is relevant to the geochemical features of intrusives. These features are further testified by remarkable occurrence of titanomagnetite in the intrusives belonging to magnetite-type granites. Molybdenum is hosted by high temperature molybdenite veinlet within intrusives and thus does not represent any correlation with other elements related to an epithermal and low temperature setting (Arjmandzadeh *et al.*, 2010).

Cluster Analysis Diagram (CA):

The CA, consists of various algorithms and approaches applied to classify the options into identical groups. Namely, it is an analytical approach aiming at organizing variables into groups in a way that correlation is maximized. The common outcome of CA is Tree Diagram (Hill *et al.*, 2006). Cluster Tree dovetails the identical options, producing a larger cluster, assessing likeness among the samples (Anazawa *et al.*, 2004; Nguyen *et al.*, 2005). The dendrogram resulted from the cluster analysis of metals is presented in Figure. 5. The diagram entails three chief branches. The 1st branch entails Cu, Sn, Cr, Zn, Pb, Ni, Mg, Mn, Fe and Cr. The branch is subdivided into Zn, Fe, Mn, Ni and Mg or into Sn, Pb. Most portion of natural Cr, commonly, lies within different minerals and, at times, is associated with Al and Fe, all depending upon the closed network grid forms

(Avudainayagam *et al.*, 2003). This fact can explain the obtained coefficient of correlation for Cr and Fe ($r=0.9$). The correlation coefficient between Cr and Mg is $r=0.89$, as well. In aerobic and anoxic conditions, Cr(III) slowly converts to Cr(VI) in the presence of Mn-oxides (Bartlett & James, 1979). This is the reason for strong correlation between Cr and Mn.

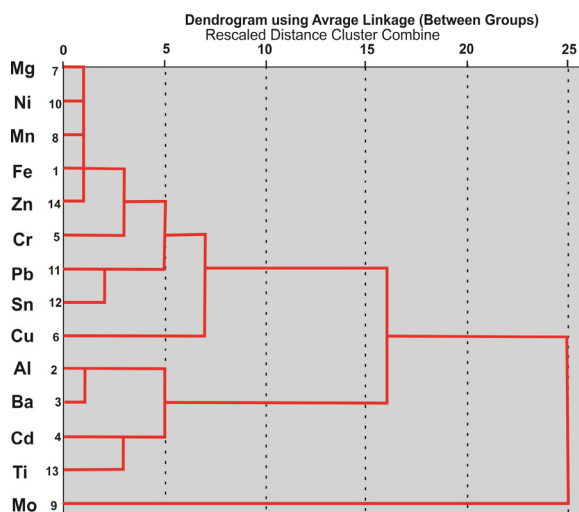


Figure 5: Dendrogram resulted from the cluster analysis of elements in soil samples from Chah-Shaljami polymetal ore deposit.

As mentioned before when calculating Pierson's coefficient of correlation (Table 2), Ni has strong correlation with Fe and Mg ($r=0.955$, $r=0.977$) and are grouped in the same cluster. Additionally, Mn and Fe are specified by the same cluster.

Table 2. Pierson's coefficient of correlation for elements in soil samples from Chah-Shaljami polymetal ore deposit.

	Cd	Cr	Cu	Fe	Mg	Mn	Mo	Na	Pb	Sn	Ti	Zn	Al	Ba	As	Ca	Co	Na	V	Sr
Cd	1																			
Cr	.357	1																		
Cu	-.191	.554*	1																	
Fe	.098	.900**	.565*	1																
Mg	.151	.858**	.574*	.957**	1															
Mn	.152	.890**	.610*	.962**	.975**	1														
Mo	-.250	-.460	-.183	-.264	-.231	-.289	1													
Ni	-.001	.826**	.633**	.955**	.977**	.977**	-.193	1												
Pb	.039	.674**	.682**	.712**	.773**	.795**	-.314	.680**	1											
Sn	.269	.711**	.668**	.685**	.769**	.747**	-.457	.534*	.877**	1										
Ti	.838**	.739**	.182	.542*	.577	.593*	-.489	.258	.433	.627**	1									
Zn	.169	.894**	.776**	.918**	.945**	.958**	-.309	.853**	.839**	.844**	.606*	1								
Al	.812**	0.288	-.147	0.110	0.235	0.125	-.228	0.033	0.074	0.391	.744**	0.189	1							
Ba	.835**	0.111	-.265	-.093	0.024	-.071	-.181	-.180	-.077	0.250	.669**	-.002	.962**	1						
As	-.226	0.175	0.050	0.435	0.446	0.315	0.200	0.395	0.073	0.202	0.024	0.264	0.163	0.038	1					
Ca	0.223	0.876**	0.543*	0.964**	0.983**	0.968**	-.0198	.952**	.746**	.743**	.625**	.932**	0.252	0.065	0.418	1				
Co	-.031	0.653**	0.632**	0.850**	0.831**	0.860**	-.0121	.923**	.660**	0.497	0.115	.795**	-.0322	-.510*	0.339	.794**	1			
Na	-.0197	0.756**	0.633**	0.932**	0.882**	0.911**	-.0130	.946**	.680**	.534*	0.258	.853**	-.0209	-.0401	0.385	.870**	.967**	1		
V	0.848**	0.665**	0.037	0.451	0.447	0.443	-.528*	0.290	0.289	.535*	.953**	0.456	.798**	.743**	0.034	.506*	-.031	0.130	1	
Sr	-.0762	-.0713	-.0201	-.0584	-.0655	-.0600	0.344	-.503*	-.0458	-.677**	-.922**	-.638**	-.832**	-.703**	-.0268	-.672**	-.0145	-.0294	-.881**	1

** Correlation is significant at the 0.01 level (2-tailed).
* Correlation is significant at the 0.05 level (2-tailed).

Mn-oxides can settle concurrently with Fe-oxides, dumping in horizons rich in oxides and hydroxides of Fe (He *et al.*, 1998). On the other hand, studies show that Mn-oxides have the greatest tendency to absorb Pb (Kabata-Pendias, 1980). Consequently, these metals are grouped in the 1st cluster. The 2nd cluster consisted of Ti, Cd, Ba and Al in which relationship between Al and Ba and between Cd and Ti is further intimate. Eventually, the 3rd branch consists of molybdenum which displays no meaningful relationship with other elements. This is, also, verified by the Pierson's coefficient of correlation measured for these elements.

Principal Component Analysis (PCA):

Since different processes take part in trapping heavy metals in various geochemical phases, the significance of multi-dimensional geostatistical approaches is evident. One of the multi-variable analysis is the (PCA) Principal Component Analysis or Factor Analysis (FA) are multi-variable geostatistical approaches which seek a linear combination of variables such that the maximum variance is extracted from the variables. Therefore multivariate methods are employed to detect, analyze and visualize the interactions between geochemical processes and environmental variables. Moreover, PCA has been used to distinguish the parental compositions (Yap, 2012). As displayed on Figure 6 and Table 3, the principal component analysis of a 3-component model has been suggested for the data obtained from the study area. Considering the graphic sketch, at least three different sources are presumed for the soil elements from Chah-Shaljami polymetal ore deposit. The 1st component includes Ni, Mg, Mn, Fe, Cr, Cu, Sn, Zn and Pb. This elemental composition and their relationship of correlation are further documented by the Pierson's coefficient of correlation and Dendrogram.

As mentioned in the Pierson's section, the source of these elements are related to the Fe, Pb and Zn mineralization in stockwork veins. The 2nd component represents Ti, Cd, Ba and Al which

indicates the occurrence of barite and sphalerite veins. The 3rd component is specified by molybdenum which generated from the intrusives and then entered the soils. Considering the polymetal nature of orebody and the investigations of Arjmandzadeh *et al.* (2010) which reported the anomaly of the heavy metals, particularly, within siliceous-sulphide vein-veinlets and stockwork zones, the positive and meaningful relationship among majority of metals is well documented.

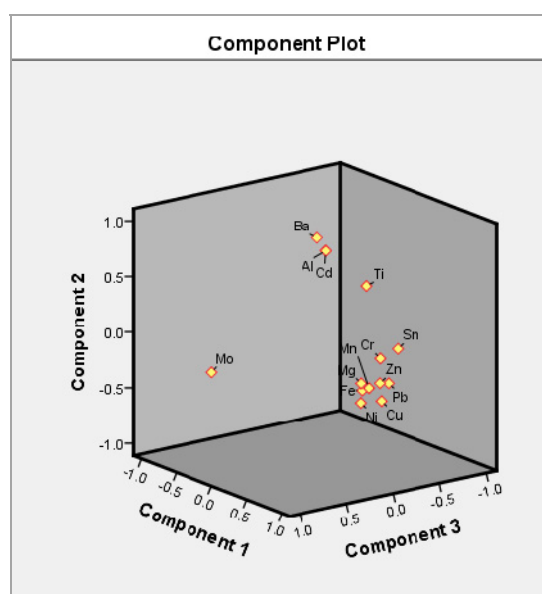


Figure 6. 3-demonsional diagram of PCA in soil samples from Chah-Shaljami polymetal ore deposit.

Contamination indices studies:

A miscellany of indices are at hand to assess soil quality in terms of contamination coefficient, land zoning and enrichment indices (Adamo *et al.*, 2005; Reddy *et al.*, 2004). The geochemical and environmental contaminations induced by heavy metals in the region are investigated as follows:

Enrichment Factor (EF):

This is a key factor, in environmental analyses, in assessment of the degree of concentration of elements triggered by anthropogenic and natural factors (Lu *et al.*, 2009).

Table 3: Results of Principal Component Analysis

		Al	Ba	Cd	Cr	Cu	Fe	Mg	Mn	Mo	Ni	Pb	Sn	Ti	Zn
Component	1	0.311	0.124	0.291	0.928	0.665	0.921	0.95	0.957	-0.414	0.914	0.842	0.879	0.715	0.979
	2	0.893	0.956	0.889	0.056	-0.428	-0.197	-0.121	-0.175	-0.248	-0.309	-0.215	0.088	0.654	-0.145
	3	0.114	0.068	0.101	-0.001	-0.212	0.186	0.22	0.142	0.797	0.197	-0.156	-0.226	-0.013	0.042

The EF is an opposite instrument to identify the lithogenic and anthropogenic resources of metals. The factor is, illustrated in the following relation: Equation 1:

$$EF = \frac{(X/Al)_{sediment}}{(X/Al)_{crust}}$$

Where X is Expected concentration and Al is the element that has not been affected by the geology of the area, being invoked in normalization process (Abdallah, 2007). Reference element is referred to element which has a thoroughly geological provenance. On environmental studies, elements like Zr, Ti, Fe, Al and Sc are of further application as reference elements among their counterpart elements (Abraham & Parker, 2008). The enrichment factor can be viewed, based on classification proposed by sutherland (2000) (Sutherland, 2000), as follows:

Table 4. Contamination categories based on enrichment factor (EF) values (after

EF	Contamination categories
<2	Deficient to minimal enrichment
2-5	Moderate enrichment
5-20	Significant enrichment
20-40	Very high enrichment
>40	Extremely high enrichment

Imperceptible amounts of enrichment might be related to discrepancy in composition of indigenous soils, or to the kind of reference element. The imperceptible amounts would not cause remarkable contamination (Kartal *et al.*, 2006). In this study, the EF of heavy metals found in soil samples, has been measured in terms of the average amount of elements in earth crust (Table 5). Results are as follows:

The highest amounts of EF indicates S, based on Chen *et al.* (2007) (Chen *et al.*, 2007). This

enrichment falls within the highest extent. Considering the very extensive sulphide minerals occurrences in the area, enrichment of sulphur seems to be relevant. The very extensive occurrence of Sulphur in soils results from very extreme alteration and weathering. Pb, Mn, Mg, Sb show extreme, relatively extreme and medium enrichment. Studies by Arjmandzadeh *et al.* (2010) also is an approval to the heavy metal anomalies such as Zn, Pb, Sb, As and Cu within siliceous, sulphide and stockwork veins. In epithermal ore deposits, antimony is commonly associated with Au, As, Pb and S and incorporating into more than 100 minerals (Zhu *et al.*, 2011). Perhaps, the enrichment of antimony is due to its association with S. Considering EF<10 for these elements, their lithogenic is confirmed (Devesa-Rey *et al.*, 2009).

Geoaccumulation index

The geoaccumulation index (Igeo) was proposed by Muller (1969) to assess heavy metal contamination of sediments and it builds on the background level of natural fluctuations including very low anthropogenic input.. The index marks extremity of anthropogenic factors (Anagnostou *et al.*, 1997). It is invoked to determine the level of contamination and can be reached via the following relation:

Equation 2:

$$I_{geo} = \log 2 \left(\frac{C_n}{1.5 B_n} \right)$$

Where Cn is the measured concentration of the element in the pelitic sediment fraction (<2 µm) and Bn is the geochemical background value in fossil argillaceous sediment (average shale).

The index tabulates soils into 6 groups in terms of contamination level (Muller, 1969) (Table 6). The geoaccumulation index is measured based on equation 2 and of the metal background concentration in shale. The results obtained for these elements are represented in the histogram (Figure. 7).

Table 5. EF and average presence of elements in the earth crust (from US Environmental Protection Agency (Harikumar *et al.*, 2009; Turekian & Wedepohl, 1961))

Element	Al	Cd	Co	Cr	Cu	Fe	Mg*
EF	1	4.71	0.74	1.17	1.11	1.05	7.6
Earth Crust (Avg.)	82300	0.2	25	102	55	41000	2350
Element	Mn*	Mo	Ni	Pb	S**	Sb**	Zn
EF	6.68	1.04	1.13	2.68	74.84	15.27	1.3
Earth Crust (Avg.)	100	1.5	50	12.5	100	0.2	70

Considering the Figure. 7 and Table 6, the most frequent class lies in group 1.24. Based on the Muller (1969) classification, although, the extremity of contamination in the soils of Chah-Shaljami polymetal ore deposit lies entirely within the non-contaminated area, and only Cd and S with goeaccumulation index of 1.24 and 0.049 and level 1 contamination reflect low levels of contamination, but generally, the Chah-Shaljami soils are considered as non-contaminated area in an environmental point of view. The following map represents distribution of S contamination in terms of goeaccumulation index (Figure 8).

Table 6. Values of the goeaccumulation index to measure soil contamination degree (after Muller (1969))

I geo	Class	The value of the pollution level
<0	0	Unpolluted
0-1	1	Unpolluted to moderately polluted
1-2	2	Moderately polluted
2-3	3	Moderately to strongly polluted
3-4	4	Strongly polluted
4-5	5	Strongly to extremely polluted
>5	6	Extremely polluted

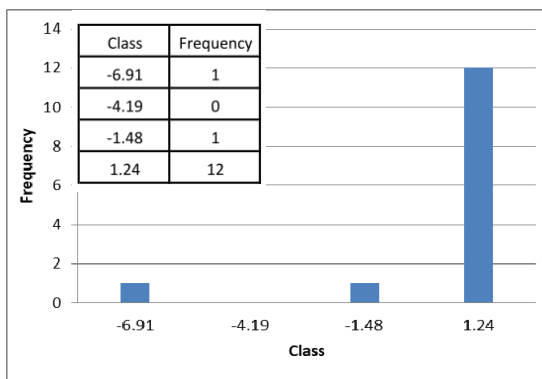


Figure 7. Histogram of geoaccumulation index values.

Contamination Factor (Cf)

The assessment of soil contamination was also carried out using the contamination factor (Cf). Contamination factor is ratio of the concentration of the element in samples to pre-industrial reference value for the element (Table 7).

The factor is invoked to determine the contamination of soil by heavy metals. This evaluates the degree of concentration of elements vis-à-vis natural values, Figureing soil contamination degree. The factor works as follows:

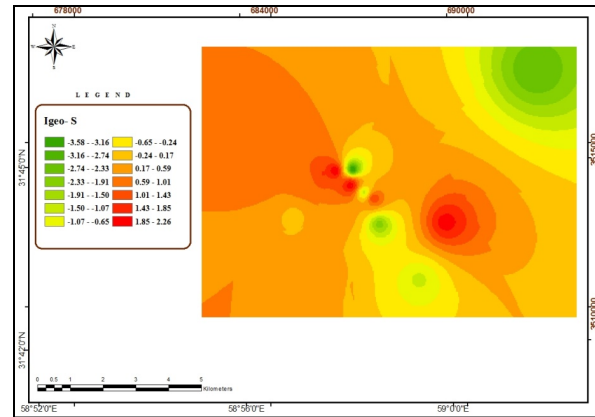


Figure 8. Distribution map of S contamination in soil sample of Chah-Shaljami polymetal ore deposit based on the goeaccumulation index.

Equation 3

$$Cf = (C_{metal} / C_{background})$$

Where C_{metal} is the mean content of metals from at least five sampling sites and $C_{background}$ is the pre-industrial.

Table 7. The assessment of contamination by heavy metals based on Cf (Hakanson, 1980).

CF	Description
CF<1	Low degree of contamination
1<CF<3	Moderate degree of contamination
3<CF<6	Considerable degree of contamination
CF>6	Very high degree of contamination

The reference concentration for shale is universally accepted. The results can be assessed considering data represented on Figure. 9. The most abundant data setting falls in 1.273, which indicates medium contamination based on Hakanson’s classification (1980) (Hakanson, 1980). Considering the Cf values, the Cd contamination level is considerably high, but that is medium for Pb and S. typically, Pb and Zn ore deposits contain significant amounts of Cd (Alloway, 2013). Figure. 10 represents the distribution map for contamination of Cd and Pb. the medium enrichment and high Cf values for this element are possibly related to the ore deposit nature and genesis.

Other elements display little contamination, in which the contamination level can be arranged as Mg>Cr>Cu>Zn>Fe>Co>Ni>Mo. A modified and generalized form of Hakanson (1980) equation for the calculation of the overall degree of

contamination was defined as the sum of all contamination factors (Cf) for a given set of pollutants divided by the number of analyzed pollutants just as bellow (Abraham & Parker, 2008):

Equation 4:

$$mCd = \sum_{i=1}^n \frac{Cf}{n}$$

where n is the number of analyzed elements and Cf is the contamination factor.

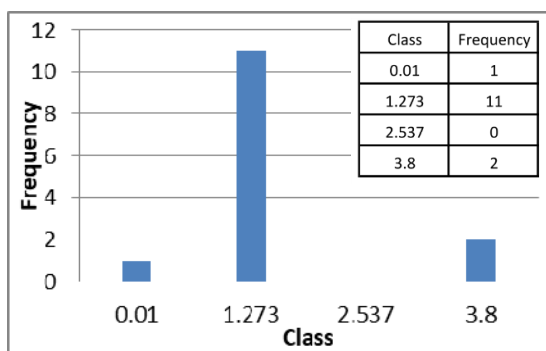


Figure 9. The histogram diagram for Cf values

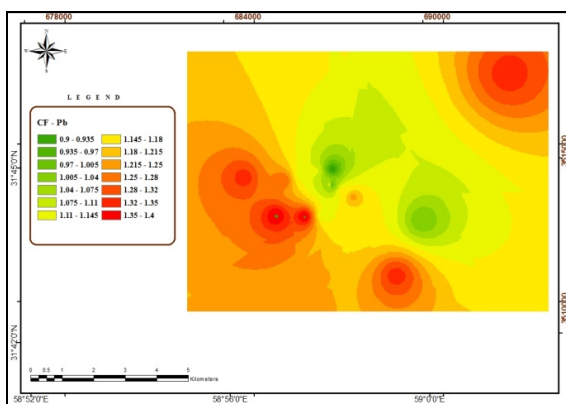
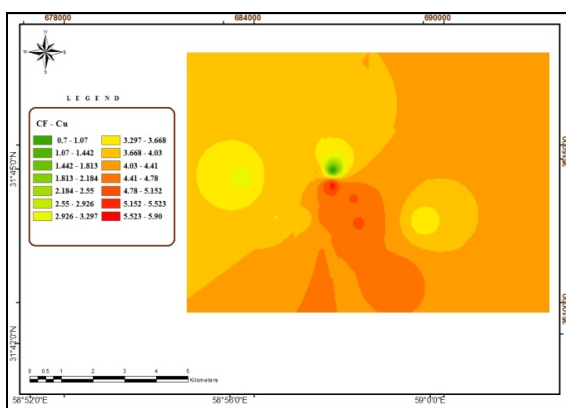


Figure 10. The contamination distribution map based on the Cf values for Cd and Pb.

Using the relation, a miscellany of heavy metals can be investigated with no restrictions. Figure. 10, represents, the contamination classification based on the modified quantification degrees of Cf (mCd) by Abraham&Parker (2008) (Table 8). Figure 11 represents the mCd measured in terms of Cf and Equation 4. The most abundant data setting falls within 0.1. None of the elements show considerable contamination in the area in terms of mCd and the all are considered non-contaminated.

Table 8. Different modified degree of contamination (mCd) for soil (Abraham & Parker, 2008).

mCd Class	Modified Degree of Contamination Level
mCd<1.5	Nil to very low degree of contamination
1.5≤mCd<2	Low degree of contamination
2≤mCd<4	Moderate degree of contamination
4≤mCd<8	High degree of contamination
8≤mCd<16	Very high degree of contamination
16≤mCd<32	Extremely high degree of contamination
mCd≥32	Ultra high degree of contamination

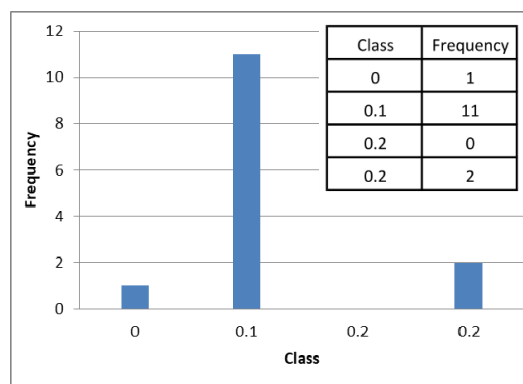


Figure 11: The histogram for modified Cf.

Conclusion

The Chah-Shaljami prospect is an extensive broadly circular alteration zone hosted by andesitic rocks. The index minerals typical of high-sulphidation epithermal deposits consisting of alunite, jarosite, chlorite, dickite, sericite, montmorillonite, quartz and Fe-oxides are detected by employing and processing ASTER data. The two soil samples are quite saline in terms of the EC measurements. The high Na, K and Mg contents of magmatic rocks have raised the EC. The positive and meaningful correlations among Fe, Mn, Mg, Ni, Pb, Zn, Cr and Sn result from Fe-bearing (e.g. pyrite, chalcopyrite and jarosite) and Pb- and Zn-

bearing mineral (e.g. galena, cerussite and sphalerite) occurrences in vein-veinlets and stockwork zone. On the Cluster Analysis Diagram, the positive correlation among Ti, Cd, Ba and Al is relevant to the occurrence of barite and sphalerite veins and geochemical features of intrusives. In the principal component analysis, the 3rd branch consists of molybdenum which displays no meaningful relationship with other elements. Molybdenum is hosted by high temperature molybdenite veinlet within intrusives and thus does not represent any correlation with other

elements. While anomalous amounts of Pb, Mn, Sb, S are detected, the geoaccumulation index represents low level of contamination by Cd and S. Considerable contamination by Cd and medium by Pb and S are substantiated by contamination factor. Finally, considering the polymetal nature of Chah-Shaljami orebody and the occurrence of siliceous-sulphide vein-veinlets and stockwork zones, the positive and meaningful relationship among majority of metals and their lithogenic sources are well documented.

References

- Abdallah, M., 2007. Accumulation and distribution of heavy metals in surface sediments of a semi enclosed basin in the southeastern Mediterranean sea, Egypt. *Mediterranean Marine Science*. 8: 31-40.
- Abraham, G., Parker, R., 2008. Assessment of heavy metal enrichment factors and the degree of contamination in marine sediments from Tamaki Estuary, Auckland, New Zealand. *Environmental monitoring and assessment*. 136: 227-238.
- Adamo, P., Arienzo, M., Imperato, M., Naimo, D., Nardi, G., Stanzione, D., 2005. Distribution and partition of heavy metals in surface and sub-surface sediments of Naples city port. *Chemosphere*. 61: 800-809.
- Alloway, B.J., 2013. Sources of heavy metals and metalloids in soils, *Heavy metals in soils*, Springer, p. 11-50.
- Anagnostou, C., Kaberi, H., Karageorgis, A., Environmental impact on the surface sediments of the bay and the gulf of Thessaloniki (Greece) according to the geoaccumulation index classification, *in Proceedings International conference on water pollution 1997*, p. 269-275.
- Anazawa, K., Kaida, Y., Shinomura, Y., Tomiyasu, T., Sakamoto, H., 2004. Heavy-metal distribution in river waters and sediments around a "Firefly Village", Shikoku, Japan: application of multivariate analysis. *Analytical Sciences*. 20: 79-84.
- Arjmandzadeh, R., Karimpour, M., Mazaheri, S., Santos, J., Medina, J., Homam, S., 2010. Investigation of alteration zones, geochemistry and petrogenesis of the Chahshaljami prospect, Eastern Iran. *Iranian journal of Researches in Earth Sciences*. 1: 74-89.
- Arjmandzadeh, R., Karimpour, M.H., Mazaheri, S.A., Santos, J., Medina, J., Homam, S.M., 2011. Sr-Nd isotope geochemistry and petrogenesis of the Chah-Shaljami granitoids (Lut block, eastern Iran). *Journal of Asian Earth Sciences*. 41: 283-296.
- Arjmandzadeh, R., Santos, J., 2014. Sr-Nd isotope geochemistry and tectonomagmatic setting of the Dehsalm Cu-Mo porphyry mineralizing intrusives from Lut Block, eastern Iran. *International Journal of Earth Sciences*. 103: 123-140.
- Avudainayagam, S., Megharaj, M., Owens, G., Kookana, R.S., Chittleborough, D., Naidu, R., 2003. Chemistry of chromium in soils with emphasis on tannery waste sites, *Reviews of Environmental Contamination and Toxicology*, Springer, p. 53-91.
- Bartlett, R., James, B., 1979. Behavior of Chromium in Soils: III. Oxidation 1. *Journal of Environmental Quality*. 8: 31-35.
- Chen, C.-W., Kao, C.-M., Chen, C.-F., Dong, C.-D., 2007. Distribution and accumulation of heavy metals in the sediments of Kaohsiung Harbor, Taiwan. *Chemosphere*. 66: 1431-1440.
- Devesa-Rey, R., Díaz-Fierros, F., Barral, M., 2009. Normalization strategies for river bed sediments: a graphical approach. *Microchemical Journal*. 91: 253-265.
- Febles, J., Sobrinho, N.A., López, Y.P., Zoffoli, J., Magalhães, M.L., Guedes, N., 2014. Relation among the processes of erosion-sedimentation-pollution in soils from the Distrito Pecuario "Alturas de Nazareno", Cuba. *Cuban Journal of Agricultural Science*. 48.
- Goorzadi, M., Vahabzadeh, G., Ghanbarpour, M., Karbassi, A., 2009. Assessment of heavy metal pollution in Tilehbon River sediments, Iran. *Journal of applied sciences*. 9: 1190-1193.
- Hakanson, L., 1980. An ecological risk index for aquatic pollution control. A sedimentological approach. *Water research*. 14: 975-1001.
- Harikumar, P., Nasir, U., Rahman, M.M., 2009. Distribution of heavy metals in the core sediments of a tropical wetland system. *International Journal of Environmental Science & Technology*. 6: 225-232.
- He, Z., Zhou, Q., Xie, Z., 1998. Soil-chemical balances of pollution and beneficial elements. *China Environmental Science Press*, Beijing. 276-303.

- Hill, T., Lewicki, P., Lewicki, P., 2006. Statistics: methods and applications: a comprehensive reference for science, industry, and data mining, StatSoft, Inc.
- Kabala, C., Singh, B.R., 2001. Fractionation and mobility of copper, lead, and zinc in soil profiles in the vicinity of a copper smelter. *Journal of Environmental Quality*. 30: 485-492.
- Kabata-Pendias, A., 1980. Heavy metal sorption by clay minerals and oxides of iron and manganese. *Mineral. Pol.* 11.
- Karimpour, M.H., Mazhari, N., Shafaroudi, A.M., 2014. Discrimination of different erosion levels of porphyry Cu deposits using ASTER image processing in eastern Iran: a case study in the Maherabad, Shadan, and Chah Shaljami Areas. *Acta Geologica Sinica-English Edition*. 88: 1195-1213.
- Kartal, Ş., Aydın, Z., Tokaloğlu, Ş., 2006. Fractionation of metals in street sediment samples by using the BCR sequential extraction procedure and multivariate statistical elucidation of the data. *Journal of Hazardous Materials*. 132: 80-89.
- Kluyver, H., Griffiths, R., Tirrul, R., Chance, P., Meixner, H., 1978. Explanatory text of the Lakar Kuh quadrangle 1: 250,000. *Geol Surv Iran*. 19: 1-175.
- Lu, X., Wang, L., Lei, K., Huang, J., Zhai, Y., 2009. Contamination assessment of copper, lead, zinc, manganese and nickel in street dust of Baoji, NW China. *Journal of hazardous materials*. 161: 1058-1062.
- Muller, G., 1969. Index of geoaccumulation in sediments of the Rhine River.
- Nguyen, H.L., Leermakers, M., Elskens, M., De Ridder, F., Doan, T.H., Baeyens, W., 2005. Correlations, partitioning and bioaccumulation of heavy metals between different compartments of Lake Balaton. *Science of the Total Environment*. 341: 211-226.
- Reddy, M.S., Basha, S., Kumar, V.S., Joshi, H., Ramachandraiah, G., 2004. Distribution, enrichment and accumulation of heavy metals in coastal sediments of Alang–Sosiya ship scrapping yard, India. *Marine Pollution Bulletin*. 48: 1055-1059.
- Shafaroudi, A.M., Karimpour, M.H., Stern, C.R., 2015. The Khopik porphyry copper prospect, Lut Block, Eastern Iran: geology, alteration and mineralization, fluid inclusion, and oxygen isotope studies. *Ore Geology Reviews*. 65: 522-544.
- Sutherland, R.A., 2000. Bed sediment-associated trace metals in an urban stream, Oahu, Hawaii. *Environmental Geology*. 39: 611-627.
- Turekian, K.K., Wedepohl, K.H., 1961. Distribution of the elements in some major units of the earth's crust. *Geological Society of America Bulletin*. 72: 175-192.
- USEPA, 2002, Supplemental guidance for developing soil screening levels for superfund sites, US Environmental Protection Agency, Office of Solid Waste and Emergency Response Washington, DC.
- Violante, A., Cozzolino, V., Perelomov, L., Caporale, A., Pigna, M., 2010. Mobility and bioavailability of heavy metals and metalloids in soil environments. *Journal of soil science and plant nutrition*. 10: 268-292.
- Yap, C., 2012. Application of factor analysis in geochemical fractions of heavy metals in the surface sediments of the offshore and intertidal areas of Peninsular Malaysia. *Sains Malaysiana*. 41: 389-394.
- Zhu, Y., An, F., Tan, J., 2011. Geochemistry of hydrothermal gold deposits: a review. *Geoscience Frontiers*. 2: 367-374.